TARGETING LOW-ENERGY BALLISTIC LUNAR TRANSFERS

Jeffrey S. Parker*

Numerous low-energy ballistic transfers exist between the Earth and Moon that require less fuel than conventional transfers, but require three or more months of transfer time. An entirely ballistic lunar transfer departs the Earth from a particular declination at some time in order to arrive at the Moon at a given time along a desirable approach. Maneuvers may be added to the trajectory in order to adjust the Earth departure to meet mission requirements. In this paper, we characterize the ΔV cost required to adjust a low-energy ballistic lunar transfer such that a spacecraft may depart the Earth at a desirable declination, e.g., 28.5°, on a designated date. This study identifies the optimal locations to place one or two maneuvers along a transfer to minimize the ΔV cost of the transfer. One practical application of this study is to characterize the launch period for a mission that aims to launch from a particular launch site, such as Cape Canaveral, Florida, and arrive at a particular orbit at the Moon on a given date using a three-month low-energy transfer.

INTRODUCTION

Low-energy transfers between the Earth and the Moon are receiving increased attention in recent years due to their flexibility and their potential to reduce the fuel requirements of missions to the Moon. The Artemis and GRAIL missions have demonstrated the benefits of these transfers.[1,2] The Artemis mission has been enabled by its low-energy lunar transfer since neither of its two spacecraft had the fuel needed to perform the mission using conventional trajectories. The GRAIL mission is taking further advantage of the flexibility of low-energy lunar transfers to establish a robust, 21-day launch period.

Recent studies have characterized numerous families of low-energy ballistic transfers that exist between the Earth and the Moon.[3–5] These transfers depart the Earth on different days of the month and at different departure declinations. In order to understand the practical costs and benefits of each of these transfers, one must understand the cost associated with departing the Earth from a particular orbit, e.g., from a 185 km circular LEO parking orbit at an inclination of 28.5°, in any day of a practical launch period and transferring to the Moon via each of these lunar transfers. A mission designer may then use this information to select the most practical low-energy lunar transfer for a particular mission.

Several studies are presented in this paper. The first study identifies the optimal locations to place one or two maneuvers along a transfer in order to minimize the ΔV cost needed to transfer from a particular Earth departure to a given low-energy lunar transfer. The second study permits the Earth departure conditions to vary in order to reduce the total ΔV cost of the transfer. The final study introduces a third maneuver to permit the lunar arrival conditions to vary in order to further

*Member of Technical Staff, Jet Propulsion Laboratory, California Institute of Technology, M/S 301-121, 4800 Oak Grove Dr., Pasadena, CA 91109

reduce the total ΔV cost of the transfer. The studies characterize the total ΔV required to achieve a particular low-energy lunar transfer as a function of the transfer's departure date and parking orbit inclination.

Low-Energy Lunar Transfers

The ballistic lunar transfers presented in this paper are low-energy transfers that utilize the gravitational forces of the Sun, Earth, and Moon to transfer spacecraft to the Moon using less fuel than typical Hohmann-like transfers.[3–12] They require approximately 90 days more transfer time, but $\sim$18% less ΔV than conventional lunar transfers to lunar libration orbits.[3] Two example ballistic lunar transfers are shown in Figure 1, viewed in the Sun-Earth rotating frame[13] from above the ecliptic.

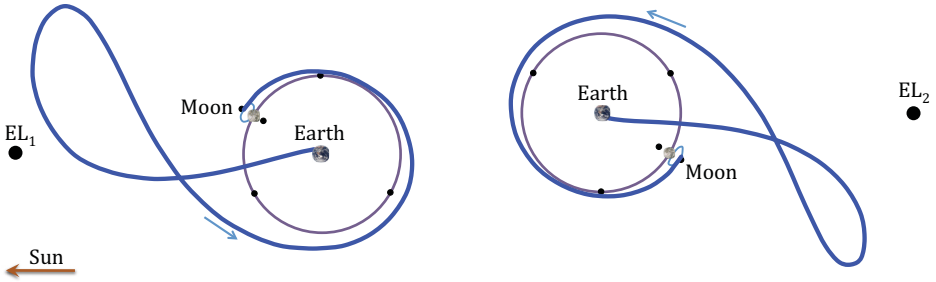

Figure 1. Two dynamical systems ballistic lunar transfers, viewed in the Sun-Earth rotating frame from above the ecliptic.

The two Artemis spacecraft are implementing different low-energy lunar transfers to insert into different lunar libration orbits;[1] this type of transfer requires no orbit insertion maneuver due to the unstable nature of lunar libration orbits and the dynamics of the Sun-Earth-Moon system.[3,14] The two GRAIL spacecraft are implementing similar low-energy lunar transfers to two low lunar orbits;[2] this type of transfer does require an orbit insertion maneuver, albeit smaller than a conventional lunar transfer's orbit insertion maneuver.[3] Both missions are able to reduce the fuel requirements of their lunar missions by implementing low-energy ballistic transfers.

Families of Transfers

A particular low-energy ballistic lunar transfer, such as either of those illustrated in Figure 1, has a set of characteristics, including its injection altitude, injection inclination, transfer duration, etc. That transfer is a member of a family of transfers, where the characteristics of each transfer in the family vary in a continuous fashion from one end of the family to the other. These families may be identified and constructed using dynamical systems methods[5] and located on a state space map, such as that shown in Figure 2.

The map shown in Figure 2 is a plot of the perigee altitude of the transfer's injection point as a function of the transfer's arrival date at the Moon and the transfer's arrival position about its target lunar orbit. Any location in the map that is colored black corresponds to a set of parameters that yields a viable low-energy lunar transfer. One can see that these black points trace out curves in the state space, corresponding to families of transfers. Figure 3 shows examples of the shapes and

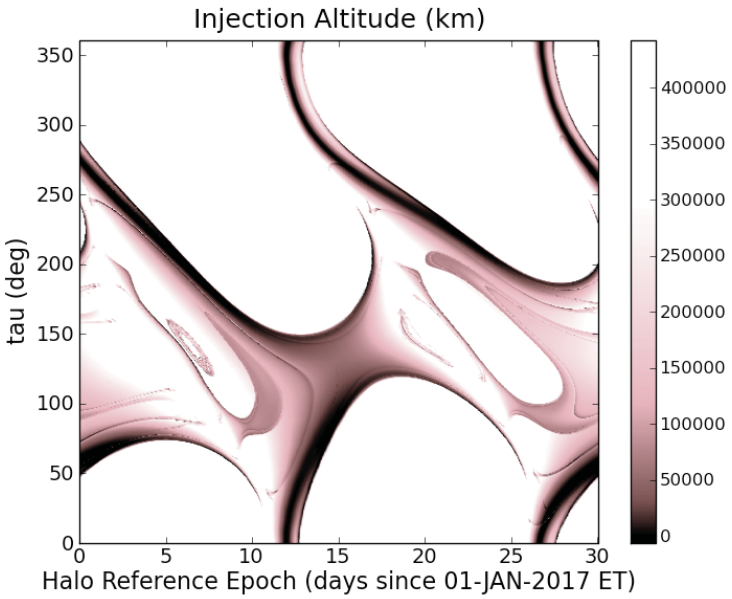

Figure 2. An example state space map that shows the injection altitude for low-energy ballistic lunar transfers to an LL_2 halo orbit as a function of their arrival date at the Moon and arrival location, τ, about the orbit.

features of these transfers and where they exist in the state space map. For more details of these families, see References 3 and 5.

The parameters of each ballistic lunar transfer in a family of such transfers vary continuously from one end of the family to the other. It may be the case that a transfer is found that departs the Earth at a desirable inclination, e.g., 28.5°, on a desirable date; but it is very unlikely that a neighboring transfer within the same family departs the Earth from the same inclination on the following day. The research presented here characterizes the ΔV cost to adjust this neighboring low-energy transfer such that it departs the Earth on the new date from the same orbital inclination.

Building a Practical Transfer

In this paper, a practical lunar transfer begins in a circular low Earth orbit (LEO) at an altitude of 185 km and an inclination of 28.5°. A trans-lunar injection (TLI) maneuver is performed that sends the spacecraft toward the Moon. The spacecraft's departure C3 may be anywhere from -2.0 to -0.3 km^2/s^2, depending on whether or not the spacecraft flies by the Moon before traversing its low-energy transfer to the Moon. The spacecraft then performs up to two deterministic trajectory correction maneuvers (TCMs) before arriving on its approach trajectory to the Moon. The approach trajectory is designed to lead the spacecraft to its destination orbit. Once the spacecraft arrives at its final destination, it may require a maneuver to enter the final orbit. If the spacecraft's final orbit is a low lunar orbit, then this maneuver is typically smaller than a conventional transfer to this orbit;[2,3] if the spacecraft's final orbit is a libration orbit, then this maneuver may be as small as a statistical correction maneuver.[3–5] See References 3–5 for more information about constructing low-energy lunar transfers to lunar libration orbits, such as halo orbits, using their stable manifolds.

The transfers in this paper are constructed in three main steps. First, a trajectory is propagated

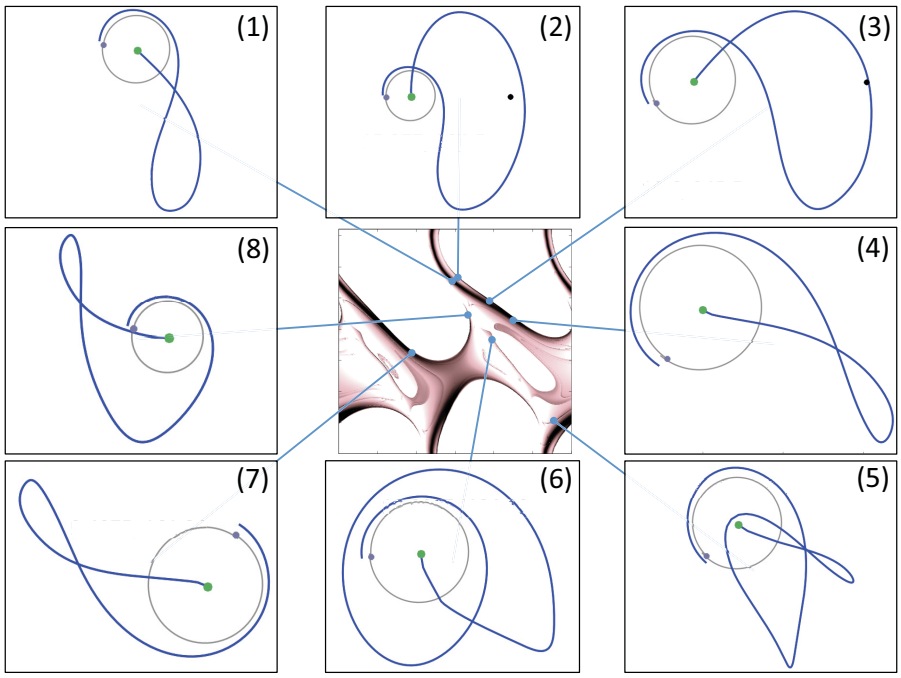

Figure 3. The state space map shown in Figure 2 reveals a wide variety of different low-energy ballistic lunar transfers, each of which exists in a family of similar trajectories.

away from the trans-lunar injection maneuver for some duration forward in time. A second trajectory is propagated backward in time away from the final desirable lunar arrival state. A third trajectory segment is constructed to connect these two trajectories via two TCMs. These three trajectory segments are summarized as follows:

Segment 1: The Earth departure segment that begins with the TLI maneuver at a 185 km low Earth orbit and propagates away from the Earth;

Segment 2: The Bridge segment, which starts with a TCM to depart Segment 1 and ends with a TCM that places the spacecraft onto Segment 3;

Segment 3: The lunar approach segment that ends at the desirable orbit about the Moon. This segment typically ends with a final maneuver to place the spacecraft into the targeted orbit.

A simple differential corrector is used to construct the Bridge segment, given the state and time of the end of Segment 1 and the beginning of Segment 3. The differential corrector determines the ΔVs that must be performed by the trajectory correction maneuvers. Details about the differential correction process may be found in References 15–17.

The final state of Segment 3 may be designed to correspond with an orbit insertion maneuver for missions that transfer to a low lunar orbit, such as GRAIL. If the transfer is designed to place the spacecraft into a libration orbit, such as Artemis, then the final state of Segment 3 may be a state along the stable manifold of that orbit.[3–5]

Optimization Software

The research presented in this paper sets up several systems of parameters and uses the software package SNOPT (Sparse Nonlinear OPTimizer)[18,19] to adjust the parameters in order to identify solutions that require minimal amounts of fuel. SNOPT is written to use a particular sequential quadratic programming (SQP) method: one that takes advantage of the sparsity of the Jacobian matrix of the constraints of the system while maintaining a quasi-Newton approximation of the Hessian of the Lagrangian of the system. The details of the algorithms are beyond the scope of this paper, except to say that they are written to be highly effective when applied to a system that has smooth nonlinear objective functions.[19]

The objective functions and constraints studied in this research are indeed nearly smooth functions. There are two reasons why the functions studied in this paper aren't perfectly smooth. First, the unstable nature of low-energy lunar transfers combined with finite-precision computers yields functions that have discontinuities. In general, these discontinuities are several orders of magnitude smaller than the trends being studied in this paper and are therefore ignored. Second, several objective functions studied in this paper involve iterative algorithms; there are discontinuities between a set of parameters that require n iterations to generate a solution and a neighboring set of parameters that require $n + 1$ iterations to converge. The discontinuities observed are small relative to the topography in the state space; thus, SNOPT tends to work well in these studies.

PROBLEM 1: BUILDING AN OPTIMAL BRIDGE

This section will study the problem of constructing an optimal bridge (Segment 2) between a given Earth departure segment (Segment 1) and a given lunar approach segment (Segment 3).

A *reference mission* has been constructed for the purposes of this study and is illustrated in Figure 4. An Earth departure segment has been constructed that departs the Earth from a low Earth orbit with the parameters shown in Table 1. This trajectory departs the Earth and nearly escapes, but rather spends some time traversing the space near the Earth under the influence of the Sun's gravity. This trajectory returns to its perigee and comes within 500,000 km of the Moon. A second trajectory has been constructed (Segment 3) that takes a similar route through space, departing the Earth from a different inclination and ultimately arriving at the Moon along the stable manifold of an LL_2 halo orbit.[3–5] The parameters of this trajectory and the lunar orbit destination are shown in Table 2. The goal of this problem is to identify the least-expensive bridge that connects the Earth-departure segment with the desirable low-energy lunar transfer.

Table 1. The parameters of the reference Earth departure, Segment 1.

Parking Orbit Parameter	Value
Altitude	185 km
Eccentricity	0.0
Inclination	28.5°
Longitude of Ascending Node	119.7°
True Anomaly	36.8°
Departure Parameter	**Value**
ΔV from Circular	3212.5 m/s
C3	–0.34206 km^2/s^2

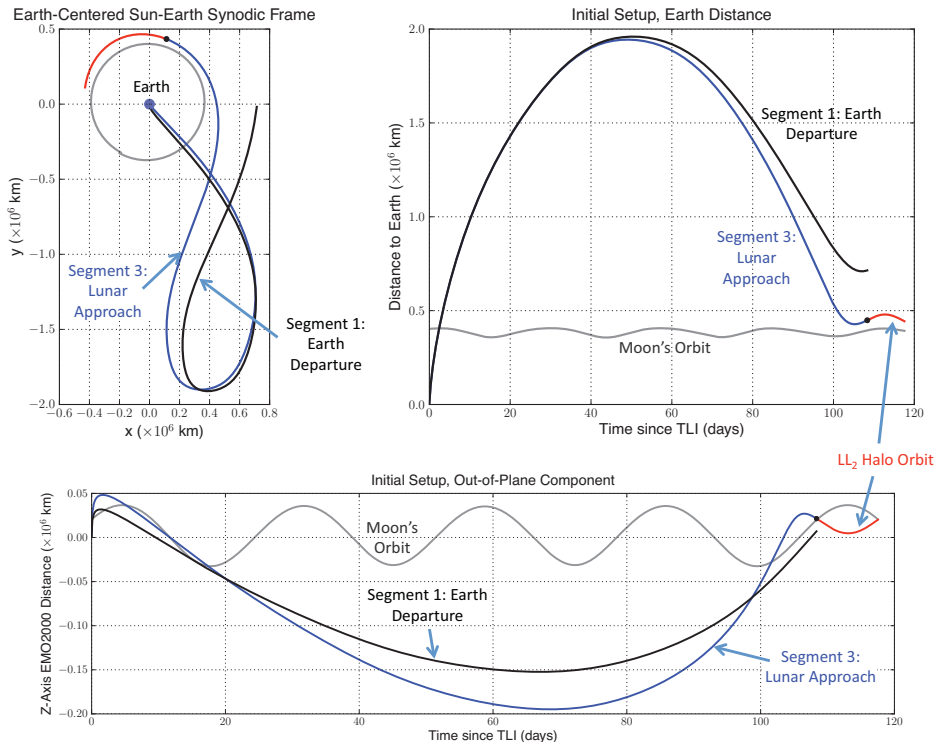

Figure 4. The reference mission for Problem 1, where an Earth-departure trajectory (Segment 1) and a low-energy lunar transfer (Segment 3) are given and the goal is to build an optimal bridge between them. Top-Left: the trajectories shown in the Earth-centered, Sun-Earth rotating coordinate frame from above the ecliptic; Top-Right: the distance between the Earth and the trajectories as a function of time; Bottom: the out-of-plane distance of the trajectories in the Earth-centered mean-ecliptic coordinate frame.

Table 2. The parameters of Segment 3, which includes the reference lunar orbit and the reference low-energy lunar transfer.

Lunar Orbit Parameter	Value
Lunar Orbit Type	Southern LL_2 Halo
Halo Reference Epoch	15 Jan 2017 12:57:36 Ephemeris Time
Halo z-axis Amplitude	30,752 km
Halo Arrival τ	287.8225°
Halo Arrival Epoch	27 Jan 2017 06:09:24 Ephemeris Time
Perigee Passage Parameter	**Value**
Epoch	01 Oct 2016 17:04:07 Ephemeris Time
Inclination	59.25°
Altitude	185 km
C3	–0.3475 km^2/s^2

Problem 1 Formulation

The first transfer problem may be summarized by listing the available controls, the required constraints, and the goals as follows:

Given: A trajectory departing the Earth (Segment 1) that begins with the TLI maneuver, and a trajectory arriving at the Moon (Segment 3) that ends with a small lunar orbit insertion maneuver.

Controls: The problem is permitted to vary the duration of Segment 1, Δt_1 (the duration of time between the TLI maneuver and TCM1), and the duration of Segment 2, Δt_2 (the duration of time between TCM1 and TCM2). The vector of control variables, $\mathbf{X_1}$, is thus equal to:

$$\mathbf{X_1} = [\, \Delta t_1,\ \Delta t_2 \,]. \tag{1}$$

Constraints: The duration of Segment 1 must be at least six days. The durations of Segments 2 and 3 must be at least two days.

Goal: Minimize the cost of the transfer, C, where $C = |\overrightarrow{\Delta \mathrm{V}}_{\mathrm{TCM1}}| + |\overrightarrow{\Delta \mathrm{V}}_{\mathrm{TCM2}}|$.

This problem will be studied first by surveying the cost of the transfer, C, for all possible placements of the two TCMs and then by exploring SNOPT's ability to find the optimal transfer quickly.

Problem 1 State Space Survey

Figure 5 shows the cost function C for each combination of placements of TCM1 and TCM2 for the reference mission illustrated in Figure 4. It's not entirely obvious, but by sampling the grid it has been determined that in this system it is optimal to place TCM1 approximately 17 days after TLI and to place TCM2 approximately 25 days after TCM1. In this case, there are approximately 75 days between TCM2 and the end of the ballistic lunar transfer, which satisfies the constraints of this problem. The total cost of the optimal transfer in this problem is approximately 29.04 m/s, where TCM1 performed approximately 25.7 m/s of the total. Figure 6 shows the optimal transfer from the same three perspectives as used in Figure 4 for comparison.

The majority of the trade space shown in Figure 5 has the desirable feature of being convex. That is, the global minimum of the transfer problem is within a basin of attraction that includes no local minima other than the global minimum. The formulation of Problem 1 described in this section has been tested on many similar transfer scenarios, connecting Earth departure segments with a variety of different low-energy lunar transfers. It has been observed that the trade space for nearly all of the tested problems includes a significant convex region. In some transfer problems there are two or three basins of attraction, which may require several tests to identify the global minimum; in other scenarios the global minima appear along a line, such that an infinite number of optimal solutions exist. This feature appears when Segments 1 and 3 intersect in position space.

Problem 1 Optimization

The survey shown in Figure 5 requires a significant amount of computation time that is typically undesirable for real-world applications. The grid shown in Figure 5 includes 160 values of Δt_1 and 160 values of Δt_2, requiring the generation of 25,600 trajectories. Furthermore, the optimal combination of Δt_1 and Δt_2 is only known within approximately 0.3 days on account of the resolution

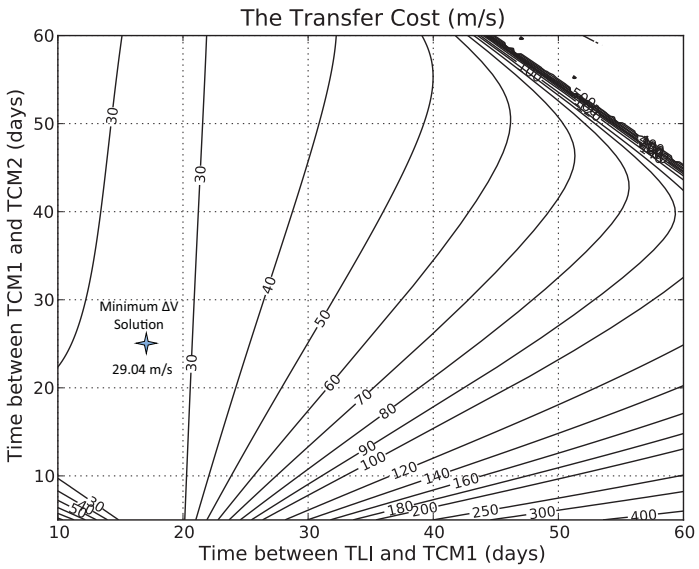

Figure 5. The cost function C for each combination of placements of TCM1 and TCM2 for the reference mission illustrated in Figure 4.

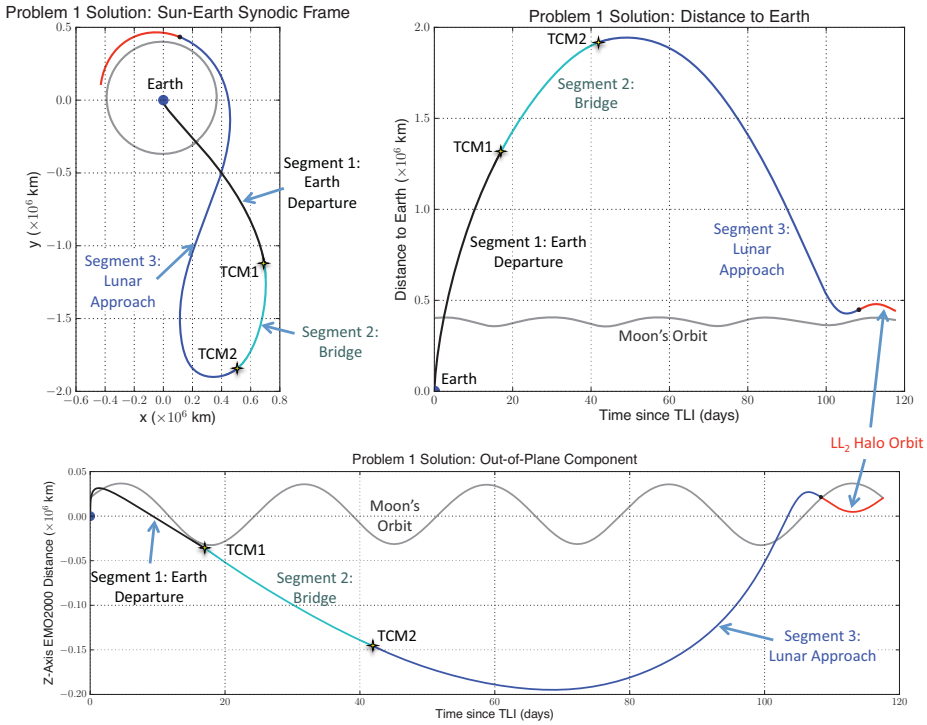

Figure 6. The optimal lunar transfer of the example Problem 1. Top-Left: the trajectories shown in the Earth-centered, Sun-Earth rotating coordinate frame from above the ecliptic; Top-Right: the distance between the Earth and the trajectories as a function of time; Bottom: the out-of-plane distance of the trajectories in the Earth-centered mean-ecliptic coordinate frame.

of the grid. An optimization algorithm such as SNOPT is typically able to converge on the optimal values far quicker and with better precision, given an initial guess within the basin of attraction of the problem. The basin of attraction for the problem shown in Figure 5 is large enough, given an appropriately tuned optimization algorithm, that most initial guesses should converge on the optimal solution quickly.

The SNOPT algorithm has been used to find the optimal solution to Problem 1 given the reference mission setup and initial guesses for $\mathbf{X_1}$ in the range of 10 days $\leq \Delta t_1 \leq$ 50 days and 5 days $\leq \Delta t_2 \leq$ 50 days. The optimizer converges on the same solution in every case. Table 3 presents an abbreviated sequence of states that the optimizer passes through on its way to convergence given one example initial state to this problem. The solution that the optimizer converges on is the same set of trajectories shown in Figure 6.

Table 3. An example set of states that SNOPT passes through as it converges on a solution to the Problem 1 formulation for the reference mission.

Iteration	Δt_1 (days)	Δt_2 (days)	ΔV_1 (m/s)	ΔV_2 (m/s)	Total ΔV (m/s)
1	20.00	20.00	27.08	2.73	29.81
5	16.41	15.90	23.10	6.00	29.10
10	17.12	24.89	25.83	3.21	29.04
15	17.00	24.92	25.70	3.34	29.04

PROBLEM 2: VARYING THE EARTH DEPARTURE

The transfer problem studied as Problem 1 assumed that Segments 1 and 3 could not be adjusted to reduce the transfer cost. This section studies the problem that permits the Earth departure to vary. It is still assumed that the trajectory departs the Earth from a circular parking orbit at an altitude of 185 km and an inclination of 28.5°, but the orientation of the orbit and the TLI maneuver magnitude may change.

Problem 2 Formulation

The second transfer problem may be summarized by listing the available controls, the required constraints, and the goals as follows:

Given: A partially constrained Earth departure trajectory (Segment 1) that begins with the TLI maneuver and a fully constrained lunar arrival trajectory (Segment 3) that ends at a desirable state near the Moon. Segment 1 originates from a circular low-Earth orbit (LEO) at an altitude of 185 km and an inclination of 28.5°; the TLI maneuver is modeled as an impulsive maneuver performed in the instantaneous velocity direction at some point along the parking orbit.

Controls: The problem is permitted to vary the following parameters:

- Ω_L: the longitude of ascending node of the LEO parking orbit;
- ν_L: the true anomaly of the location where the TLI maneuver is performed in its LEO parking orbit;
- ΔV_L: the magnitude of the TLI maneuver;

- Δt_1: the duration of Segment 1, i.e., the duration of time between the TLI maneuver and TCM1; and
- Δt_2: the duration of Segment 2, i.e., the duration of time between TCM1 and TCM2.

The vector of control variables, $\mathbf{X_2}$, is thus equal to:

$$\mathbf{X_2} = [\, \Omega_L,\ \nu_L,\ \Delta \mathrm{V}_L,\ \Delta t_1,\ \Delta t_2\,]\,. \tag{2}$$

Constraints: The TLI maneuver is performed at a given time, at an altitude of 185 km, at an inclination of 28.5°, and in the velocity direction; the duration of Segment 1 must be at least six days; the durations of Segments 2 and 3 must be at least two days.

Goal: Minimize the cost of the transfer, C, where $C = |\overrightarrow{\Delta \mathrm{V}}_{\mathrm{TCM1}}| + |\overrightarrow{\Delta \mathrm{V}}_{\mathrm{TCM2}}|$. The magnitude of the TLI maneuver is not included in the cost function.

The optimization algorithm SNOPT has been used once again to find a solution to this problem. It has been found that SNOPT readily converges on a good solution to this problem when the initial guess is within the basin of attraction of a good local minimum, if not the global minimum. An algorithm is described next that generates a good initial guess quickly. The basin of attraction is very large for trajectories that do not include an outbound lunar flyby. Lunar flybys increase the sensitivity of the problem and dramatically reduce the basin of attraction of the optimizer. As such, they are out of the scope of this study.

Problem 2 Constructing an Initial Guess

The second transfer problem has five control variables, given as $\mathbf{X_2}$ in Equation 2, including three parameters that define the initial state of Segment 1 (Ω_L, ν_L, and $\Delta \mathrm{V}_L$) and two parameters that describe when to perform the TCMs. It has been found that a four-step process may be used to generate a good initial guess of $\mathbf{X_2}$. This process is broken into four steps so that the entire process has a high probability of ending near a global minimum rather than one of many local minima that occur in the state space. Table 4 provides an example progression of $\mathbf{X_2}$ through these steps for the case of the reference mission described in this paper.

The first step is to generate an initial estimate for Segment 1 that places the final position of Segment 1 beyond the orbit of the Moon. This eliminates most local minima in the state space. In most circumstances, Segment 1 travels well beyond the Moon's orbit after about six days. The main exceptions involve situations where Segment 1 is designed to fly past the Moon one or more times, with optional large Earth staging orbits. These exceptions are beyond the scope of this study since they require very different optimization schema. In this study Δt_1 is initially set to 20 days and the parameter $\Delta \mathrm{V}_L$ is set to a value that places the end of Segment 1 at the same distance from the Earth as Segment 3 is at the same time. The $\Delta \mathrm{V}_L$ value applied to the low-Earth parking orbit is typically equivalent to an injection energy C3 in the range of -0.6 km^2/s^2 to -0.3 km^2/s^2.

The next step is to orient this departure trajectory in such a way as to minimize the position difference between the final position of Segment 1 and the position of Segment 3 at the same time. It has been found that SNOPT converges very quickly on values for the parameters Ω_L and ν_L when the goal is to minimize this position difference.

Once initial estimates are obtained for Ω_L and ν_L, then another optimization run is initiated to permit all three parameters Ω_L, ν_L, and $\Delta \mathrm{V}_L$ to vary in order to fine-tune the initial guess of $\mathbf{X_2}$

to minimize the position difference at the end of Segment 1. It is often the case that SNOPT can reduce this position difference to machine precision if requested, which makes sense since there are three control variables and three constraints, provided that a 28.5° inclination LEO parking orbit can reach the target position.

The fourth and final step is to adjust Δt_1 and Δt_2, if needed. The state space survey of Problem 1 demonstrates that a good guess for Segment 1 results in a large basin of attraction for Δt_1 and Δt_2. In this study, Δt_1 and Δt_2 are both set to 21 days, where this value is intentionally slightly different than the initial estimate for Δt_1. It has been observed on numerous occasions that if the initial estimate of $\mathbf{X_2}$ is set up such that the position difference between Segments 1 and 3 is nearly zero at the time of one of the TCMs, then the optimizer has a difficult time getting away from that solution. After some surveying, it has been found that this is a situation where the initial guess places the optimizer into a gully in the state space, where the cost function is nearly flat. It has been found that it is better to place the initial guess of $\mathbf{X_2}$ slightly off of this flat area, even if doing so hurts the optimization objective function. Setting Δt_1 to 21 days instead of 20 days, namely at least one day away from the time that Segment 1 and Segment 3 nearly intersect, is sufficient to do that. More details of this issue may be found in the Appendix.

Table 4. An example of the process of constructing an initial guess of $\mathbf{X_2}$ for the reference mission described in this paper.

Step	Ω_L (deg)	ν_L (deg)	ΔV_L (m/s)	Δt_1 (days)	Δt_2 (days)	Notes
0	0°	0°	3200	20	-	Initialization
1	0°	0°	3207.45	20	-	Target C3 ~ -0.4532 km^2/s^2
2	120.50°	35.39°	3207.45	20	-	Adjust Ω_L and ν_L
3	119.64°	36.71°	3212.52	20	-	Adjust Ω_L, ν_L, and ΔV_L
4	119.64°	36.71°	3212.52	21	21	Final Adjustments

Problem 2 Optimization

We are now prepared to run the full SNOPT optimization. The first test of this optimization scheme will be on the same reference mission studied in Problem 1 and illustrated in Figures 4 and 6. The target lunar approach trajectory (Segment 3) is precisely the same trajectory, however, now the Earth departure segment is permitted to change.

Table 4 provides the initial guess that is used to initialize the optimizer. The initial values of Ω_L, ν_L, and ΔV_L are slightly different than those studied in Problem 1. If one surveys the state space of the cost function for Problem 1 given this new set of parameters, one finds that the state space is still nearly identical to that shown in Figure 5. It is reassuring knowing that at least two dimensions of the parameter-space are convex.

Table 5 presents an abbreviated sequence of states that the optimizer passes through as it converges on a solution to the reference mission given the initial state shown in Table 4. One can see that the initial guess of $\mathbf{X_2}$ is very similar to the converged state and the optimizer converges quickly on the solution.

The solution to Problem 2 applied to the reference mission requires quite a bit less ΔV than the solution to Problem 1. Table 6 compares the solution parameter sets. It's interesting to notice that the final, converged solution to Problem 2 yields a set of trajectories that require only one deterministic

Table 5. An example set of states that SNOPT passes through as it converges on a solution to the Problem 2 formulation for the reference mission.

Iter. #	Ω_L (deg)	ν_L (deg)	ΔV_L (m/s)	Δt_1 (days)	Δt_2 (days)	ΔV_1 (m/s)	ΔV_2 (m/s)	Total ΔV (m/s)
1	119.64	36.71	3212.52	21.00	21.00	29.64	1.38	31.02
4	119.43	36.61	3212.52	20.66	21.02	25.89	3.99	29.88
10	119.36	36.95	3212.52	20.46	21.00	26.69	1.05	27.74
20	115.88	39.96	3212.73	22.81	22.52	3.72	17.83	21.54
30	115.57	40.12	3212.79	22.86	22.83	0.10	19.48	19.58
50	114.28	41.34	3212.88	27.90	28.42	0.01	18.58	18.59
70	114.24	41.38	3212.88	28.04	28.57	0.00	18.58	18.58

TCM. It has been found that most solutions to Problem 2 yield trajectories where either TCM1 or TCM2 has a magnitude of approximately 0 m/s and Segments 1 and 3 intersect in position space.

Table 7 summarizes the results of the optimization of several trajectories using the formulation of Problem 2. The trajectories correspond to the numbered trajectories from Figure 3; additional details have been left out for brevity. Trajectory 6 includes an outbound lunar flyby that interferes with the optimization procedure being studied. Hence, no results are presented for that trajectory. Each of the other solutions requires only a single TCM as the reference mission does.

Table 6. A summary of the parameters for the reference mission in three steps: first, the optimal solution to Problem 1 shown in Figure 6; second, the initial guess to Problem 2; and third, the converged solution to Problem 2.

Parameter	Problem 1 Solution	Problem 2 Initial Guess	Problem 2 Converged Solution
Ω_L	119.7°	119.64°	114.24°
ν_L	36.8°	36.71°	41.38°
ΔV_L	3212.5 m/s	3212.52 m/s	3212.88 m/s
Δt_1	17.00 days	21.0 days	28.04 days
Δt_2	24.92 days	21.0 days	28.57 days
TCM1 ΔV	25.70 m/s	29.64 m/s	0.0 m/s
TCM2 ΔV	3.34 m/s	1.38 m/s	18.58 m/s
Total TCM ΔV	29.04 m/s	31.02 m/s	18.58 m/s

Table 7. A summary of the TCM ΔV cost after optimizing several example transfer problems using the formulation of Problem 2. The trajectories correspond to those numbered in Figure 3.

Trajectory	TCM1 ΔV	TCM2 ΔV	Total ΔV
1	0.0 m/s	18.58 m/s	18.58 m/s
2	0.0 m/s	29.04 m/s	29.04 m/s
3	85.39 m/s	0.0 m/s	85.39 m/s
4	11.07 m/s	0.0 m/s	11.07 m/s
5	37.63 m/s	0.0 m/s	37.63 m/s
7	18.05 m/s	0.0 m/s	18.05 m/s
8	0.0 m/s	55.48 m/s	55.48 m/s

TARGETING A DEPARTURE INCLINATION

Previous studies have identified numerous families of low-energy transfers that exist between the Earth and the Moon.[3–5] Each lunar transfer in each family has a natural Earth departure declination, that is, a particular direction that permits the spacecraft to depart the Earth and arrive at the Moon without requiring a single deterministic maneuver. The optimization algorithms described in this paper provide a way to characterize the minimum ΔV needed to depart the Earth in a different direction and still arrive at the Moon along the same lunar arrival trajectory. This method is used here to characterize the expected ΔV cost needed to change the Earth departure declination a number of degrees. With that information, mission designers can estimate the cost of implementing a particular low-energy lunar transfer given that transfer's natural Earth departure declination.

In order to characterize the expected ΔV cost needed to change the Earth's departure, we will study the ΔV cost needed to transfer from LEO parking orbits in a range of inclination values onto several example low-energy transfers. In that way the optimization algorithms presented to study Problem 2 may be used to determine the least transfer ΔV needed to perform a particular transfer.

To begin this study, the trajectories involved with the reference mission studied in this paper have been optimized for a range of LEO inclination values. Figure 7 shows the optimized transfer ΔV cost for the trajectories as the inclination of the corresponding LEO parking orbit is varied from 0° to 180°. This particular low-energy transfer has a natural Earth departure declination of 59.25°, which explains why the transfer cost goes to zero at that inclination value in the plot shown in the figure. The most costly transfers involve departing the Earth from the equator; from those orbits the longitude of the ascending node cannot be adjusted and the optimizer loses a dimension of freedom.

It is interesting to consider the change in the total transfer cost as the LEO parking orbit's inclination moves away from 59.25°. The right half of Figure 7 shows this relationship. One can see that at worst it costs approximately 0.4 m/s per degree of inclination that the LEO parking orbit is changed, up to about 10 degrees of inclination change; then the trend accelerates beyond 0.5 m/s per degree of inclination change. Finally, Table 8 presents a summary of the transfer's parameter set at several points shown in the figure.

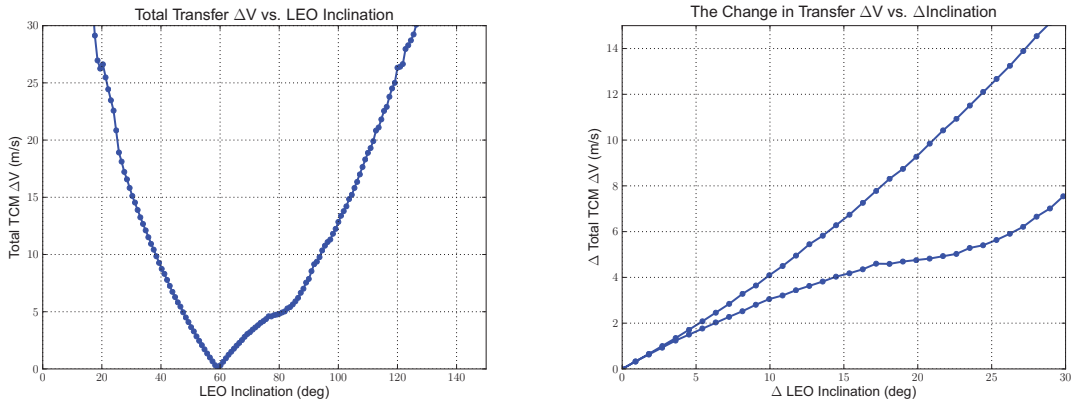

Figure 7. Left: The transfer ΔV cost for the reference mission as the LEO parking orbit's inclination is varied from 0° to 180°. Right: The change in total transfer ΔV as the LEO parking orbit's inclination changes away from the low-energy transfer's natural departure declination of 59.25°.

Table 8. The parameter set for several transfers shown in Figure 7.

LEO Inclination	Ω_L (deg)	ν_L (deg)	ΔV_L (m/s)	Δt_1 (days)	Δt_2 (days)	TCM ΔV (m/s)
20°	91.2°	62.6°	3212.99	51.3	59.4	26.62
30°	117.5°	38.0°	3212.87	46.2	57.1	15.12
40°	128.3°	29.2°	3212.68	51.6	51.7	8.74
50°	135.0°	24.4°	3212.48	52.8	50.5	3.65
60°	139.9°	21.5°	3212.23	67.0	36.1	0.33
70°	143.9°	19.8°	3211.95	57.5	45.8	3.21
80°	147.4°	18.8°	3211.63	82.3	21.1	4.82
90°	150.8°	18.8°	3211.36	81.7	21.6	7.86
100°	154.2°	19.0°	3211.13	64.1	39.2	12.85
110°	157.8°	20.3°	3211.02	63.0	40.4	18.88
120°	161.8°	22.1°	3210.90	59.1	43.0	26.32

This analysis has been repeated for several low-energy transfers. Figures 8 and 9 show the results for the trajectories labeled (4) and (7) in the plot shown in Figure 3. In each case studied, the cost needed to transfer from a particular LEO parking orbit is compared to the cost of departing from the natural LEO parking orbit and the variations are recorded as a function of the change in inclination. The slopes are observed to vary from ∼0.5 m/s per degree of inclination change up to ∼4.8 m/s per degree of inclination change. The highest slopes observed occur when the natural Earth departure declination of the low-energy transfer is very low. On average, the slope is equal to approximately 0.95 m/s per degree of inclination change.

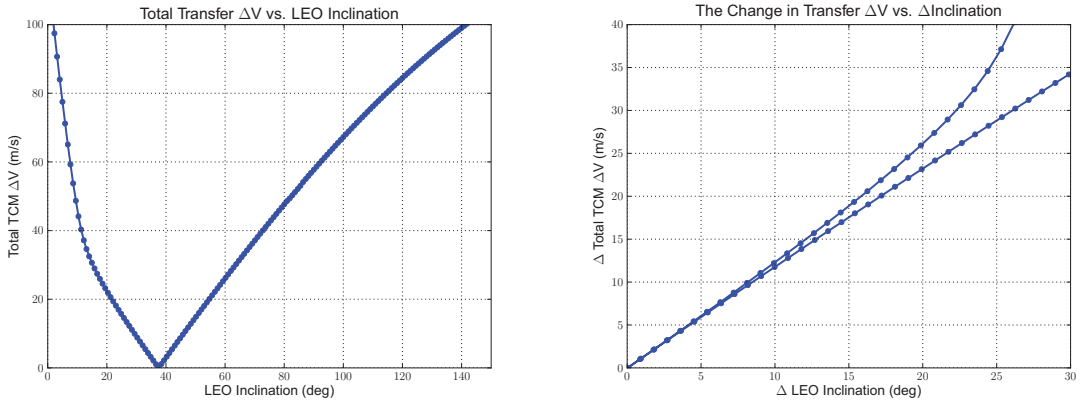

Figure 8. The same plots as shown in Figure 7, but for the low-energy lunar transfer shown as Trajectory (4) in Figure 3. This transfer's natural departure declination is 37.51°.

A mission designer can use this data to estimate the ΔV costs needed to implement a particular low-energy lunar transfer from a particular LEO parking orbit by comparing the transfer's natural departure declination with the LEO parking orbit's inclination. The designer may estimate that it costs approximately 1 m/s for every degree of inclination change that must be corrected in the transfer using the two-maneuver scheme studied here.

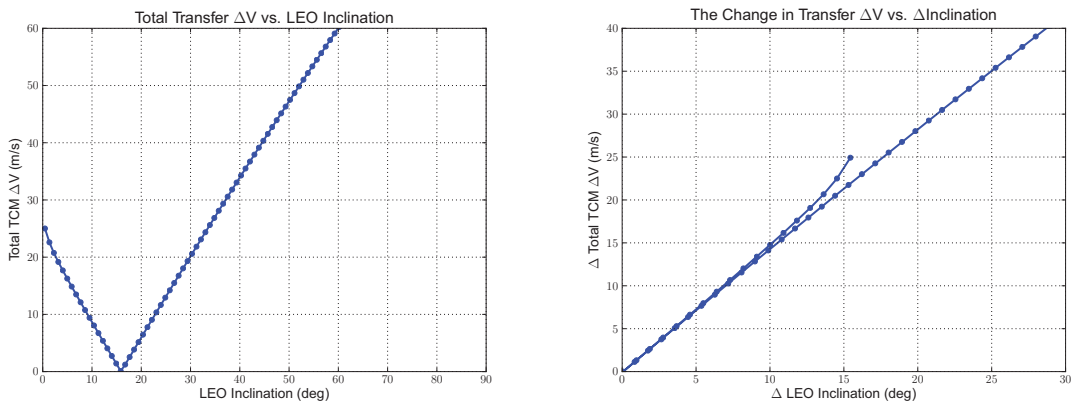

Figure 9. The same plots as shown in Figure 7, but for the low-energy lunar transfer shown as Trajectory (7) in Figure 3. This transfer's natural departure declination is 15.89°.

TARGETING A DEPARTURE DATE

A given low-energy transfer propagates from the Moon backward in time until it encounters the Earth. To this point in this study, it has been assumed that the spacecraft would depart the Earth at that natural departure time. However, in reality, a spacecraft will depart the Earth at another time, which may be mere seconds away from the nominal time, or it may be days earlier or later, corresponding to different injection dates in a launch period. This section presents the ΔV costs associated with departing the Earth on a different day other than the natural departure date.

In general, the optimization algorithm described to solve Problem 2 works well when the Earth departure time is varied, although the cost of the transfer increases as one moves the injection date further from the natural date. It is hypothesized that the total transfer cost may be reduced by adding in an additional leveraging maneuver toward the end of the lunar transfer in order to adjust the duration of the transfer to coincide with the injection time. This will be studied further in the next section.

Figure 10 shows an illustration of an example scenario where the trans-lunar injection date has been shifted by 30 days relative to the low-energy lunar transfer's natural Earth departure date. This is a dramatic shift for illustration purposes; one can see that this shift causes the Earth departure trajectory and the lunar approach trajectory to differ substantially. Figure 11 shows several perspectives of the solution that the optimizer converges on using the algorithms described in this paper. The total transfer cost for this scenario is approximately 216 m/s.

Figure 12 shows the total transfer ΔV cost associated with varying the TLI date for the reference mission studied in this paper, as well as the cost that is incurred from moving away from the least-ΔV solution. One can see that the ΔV cost rises rapidly as one shifts the TLI date away from the best solution. For the case of the reference mission, the ΔV cost rises at a rate of 6 – 7 m/s per day that the TLI is shifted. Using the algorithms presented up to this point, the reference mission requires a total transfer ΔV of approximately 73.6 m/s to establish a 21-day launch period: 59.6 m/s higher than the least-ΔV injection date. Table 9 presents a summary of the transfer's parameter set at several points shown in the figure.

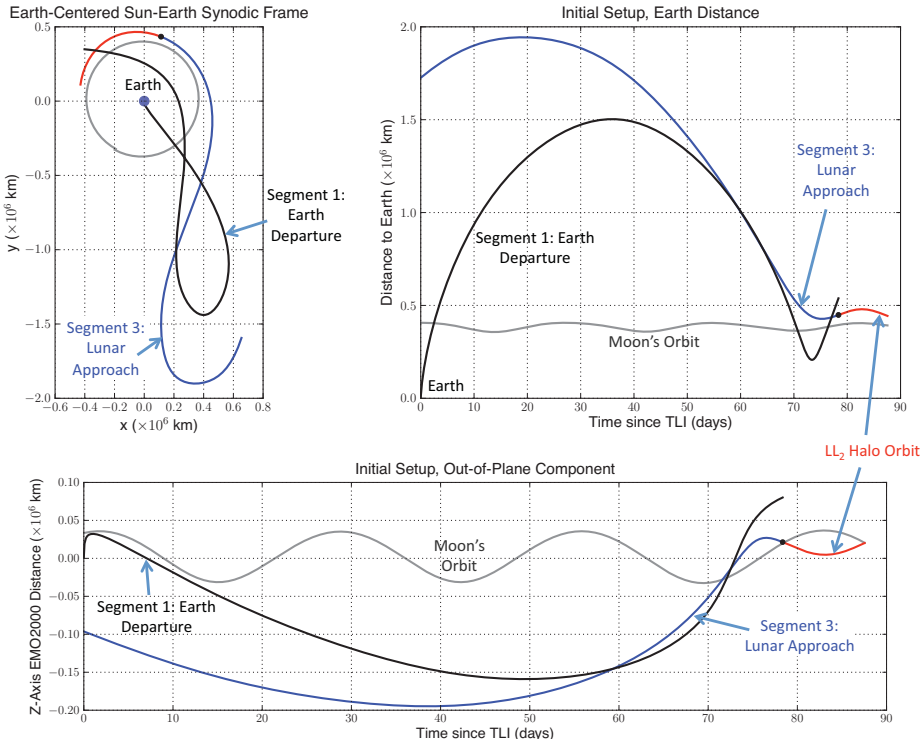

Figure 10. An example scenario where the trans-lunar injection date has been shifted by 30 days relative to the low-energy lunar transfer's natural Earth departure date. Top-Left: the trajectories shown in the Earth-centered, Sun-Earth rotating coordinate frame from above the ecliptic; Top-Right: the distance between the Earth and the trajectories as a function of time; Bottom: the out-of-plane distance of the trajectories in the Earth-centered mean-ecliptic coordinate frame.

This procedure has been applied to four other low-energy transfer problems, including trajectories 2, 3, 4, and 7 from Figure 3. The average rate of change in the mission's total transfer ΔV between these five problems has been observed to be approximately 5.3 m/s per day of change in the trans-lunar injection date.

PROBLEM 3: VARYING THE ARRIVAL CONDITIONS

When the Earth departure date is changed, it may be cost effective to introduce an additional maneuver to adjust the duration of the low-energy transfer in order to accommodate the new departure date. This will be explored as Problem 3 in this section.

There are several ways to adjust the lunar approach trajectory. It may be the case that the mission permits a transfer to arrive at the Moon on a different date. If the trajectory's destination is a low lunar orbit, the orbit insertion maneuver's ΔV magnitude, vector, and/or location about that orbit may be adjusted. If the trajectory's destination is a libration orbit, then the arrival state may be adjusted. Alternatively, in many situations a third TCM may be added to the trajectory toward the end of Segment 2.

This study assumes that the mission must arrive on a particular date and requires a particular

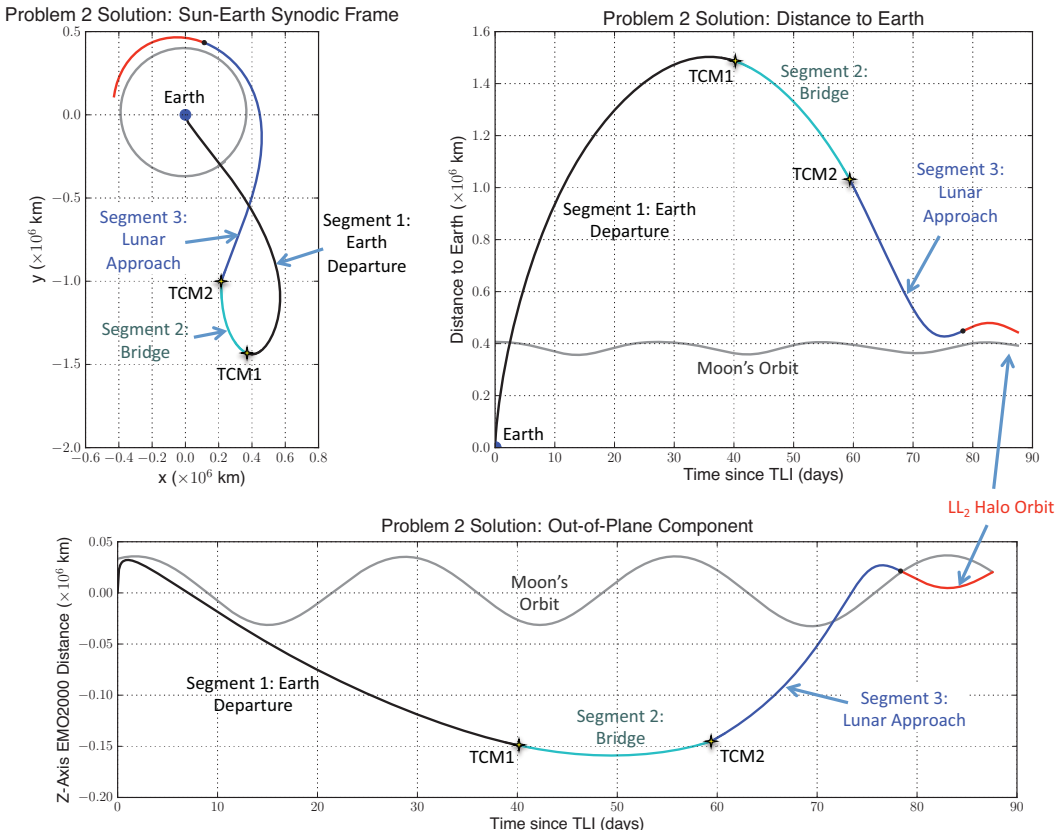

Figure 11. The optimized solution of the scenario shown in Figure 10.

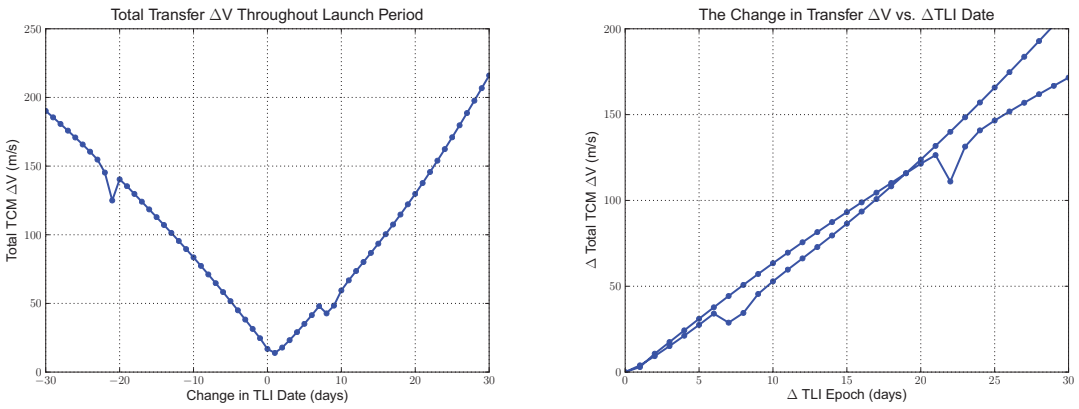

Figure 12. The transfer ΔV cost for the reference mission as the trans-lunar injection date is varied over the course of $\pm$30 days. The observed brief dips are caused by the Moon's influence as the spacecraft flies out past its orbit.

Table 9. The parameter set for several transfers shown in Figure 12.

ΔTLI Date (days)	Ω_L (deg)	ν_L (deg)	ΔV_L (m/s)	Δt_1 (days)	Δt_2 (days)	TCM ΔV (m/s)
–30	76.7°	50.6°	3217.76	52.6	70.3	190.19
–25	83.9°	49.9°	3218.68	50.8	66.8	165.75
–20	87.5°	46.2°	3212.14	45.2	67.5	140.34
–15	91.6°	49.9°	3213.55	50.3	55.9	112.82
–10	96.7°	48.7°	3211.91	50.8	49.2	83.51
–5	104.0°	46.1°	3211.99	52.3	40.9	51.66
0	115.2°	40.0°	3212.80	42.4	60.9	16.85
5	123.7°	37.6°	3213.98	51.2	33.7	35.13
10	125.4°	36.8°	3207.99	21.1	57.1	59.44
15	137.0°	30.7°	3207.97	56.6	18.6	93.52
20	144.9°	25.5°	3206.27	52.5	17.4	129.81
25	153.3°	21.0°	3206.18	47.8	17.0	170.98
30	162.5°	16.6°	3206.75	40.3	19.0	216.01

approach geometry; therefore, this study explores the costs and benefits associated with adding a third TCM (TCM3) to the transfer toward the end of Segment 2. The TCM acts as an insertion maneuver for missions to lunar libration orbits, such as those considered in this paper. The TCM places the spacecraft into the exact same lunar libration orbit, no matter the variations experienced across the launch period. This has the effect of simplifying mission planning responsibilities.

This technique is applied here using the reference mission as an example. TCM3 has been added to the reference mission trajectory approximately 10 days before the spacecraft arrives at its final state at the Moon. This location is somewhat arbitrary and it may certainly be possible to adjust its location to reduce the transfer ΔV. The location has been chosen because the trajectory has begun wrapping onto the target libration orbit in the reference mission by that time. This is approximately the point when the first station keeping may be needed as the spacecraft traverses the unstable regime near the lunar libration points; it is also the point that has been used to differentiate Segment 3 from the LL_2 halo orbit in each of the figures presented in this paper.

This new TCM introduces three new parameters to the optimization algorithm: ΔV^x_{TCM3}, ΔV^y_{TCM3}, and ΔV^z_{TCM3}. The time of the maneuver may also be varied depending on the mission requirements, but for now that variable will be excluded from the optimization problem. The remaining aspects of the problem formulation are identical to the formulation described for Problem 2. The new vector of control variables $\mathbf{X_3}$ may be described as:

$$\mathbf{X_3} = \left[\Omega_L,\ \nu_L,\ \Delta V_L,\ \Delta t_1,\ \Delta t_2\ , \Delta V^x_{\text{TCM3}},\ \Delta V^y_{\text{TCM3}},\ \Delta V^z_{\text{TCM3}} \right]. \tag{3}$$

The algorithm used to construct an initial guess for $\mathbf{X_3}$ remains the same as that described to study Problem 2; each of the TCM components is initialized at 0 m/s. The optimizer has been observed to converge quicker if the solution to Problem 2 is used as an initial guess for the appropriate elements of $\mathbf{X_3}$.

This new mission formulation has been applied to the reference mission studied in this paper. It has been found that the total TCM ΔV cost of the reference mission drops with the addition of the new TCM from 18.58 m/s to 15.11 m/s. Table 10 presents an abbreviated sequence of states that the

optimizer passes through as it converges on a solution to the reference mission. The optimization process begins with an initial state that has been constructed using the final state information shown in Table 5. The parameters Δt_1 and Δt_2 have been adjusted by 1 day each to perturb the optimizer away from the solution to Problem 2, which assists in the convergence as described in the Appendix. One can see that the optimizer converges quickly to a solution that requires less total transfer ΔV than previous solutions. Figure 13 shows the converged trajectory for illustration purposes.

Table 10. An example set of states that SNOPT passes through as it converges on a solution to Problem 3 for the reference mission. The first line is the solution to Problem 2 for reference.

Iter #	Ω_L (deg)	ν_L (deg)	ΔV_L (m/s)	Δt_1 (days)	Δt_2 (days)	ΔV_1 (m/s)	ΔV_2 (m/s)	ΔV_3 (m/s)	Total ΔV (m/s)
-	114.24	41.38	3212.88	28.04	28.57	1.34	17.42	0.00	18.58
1	114.24	41.38	3212.88	29.04	29.57	1.34	17.42	0.00	18.76
4	114.15	41.30	3212.88	29.00	29.53	3.26	13.61	0.26	17.13
10	114.07	41.07	3212.96	28.94	29.47	3.51	11.58	0.46	15.54
20	114.10	41.06	3212.97	28.18	28.27	2.42	12.26	0.59	15.26
40	114.09	40.99	3213.00	26.20	25.20	0.00	13.63	1.47	15.11

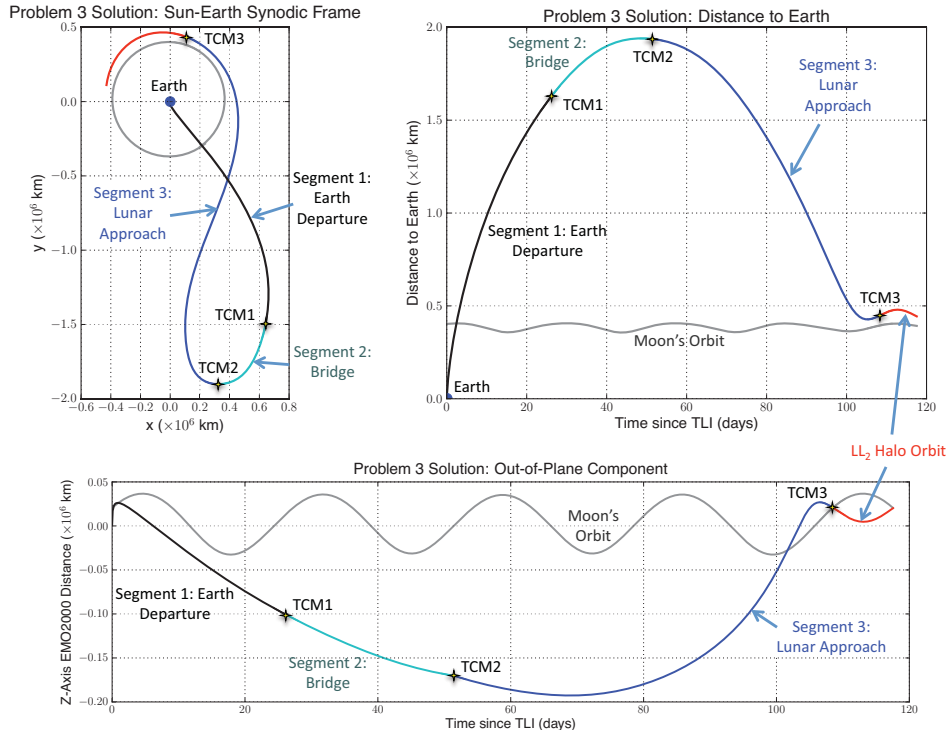

Figure 13. The solution of the reference mission optimized using the formulation of Problem 3.

CONSTRUCTING AN IMPROVED LAUNCH PERIOD

The mission formulation developed as Problem 3 has been applied to characterize the ΔV costs associated with a new launch period for the reference mission. Figure 14 shows the resulting transfer ΔV cost as a function of the change in injection date from the reference mission, where the transfer ΔV is the sum of the three TCM ΔV magnitudes. The launch period cost from Figure 12 has been superimposed to this new launch period cost. One can see that the addition of TCM3 has clearly reduced the ΔV cost in almost every launch date. A 21-day launch period requires approximately 17.6 m/s less ΔV using the three-maneuver strategy of Problem 3 than the two-maneuver strategy of Problem 2.

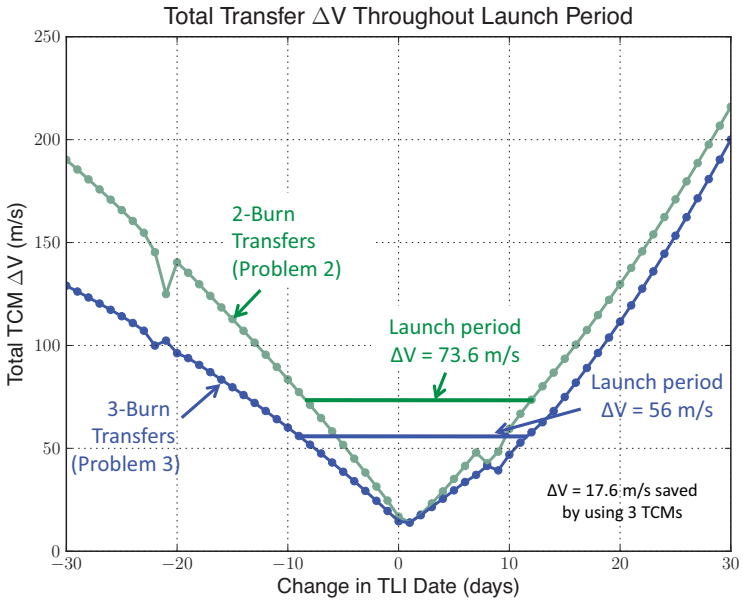

Figure 14. The total TCM ΔV cost for the reference mission as the Earth departure date is varied over the course of 60 days and the lunar arrival trajectory varies. The launch period costs shown in Figure 12 have been superimposed for reference.

It is possible that the total ΔV of the reference mission may be further reduced by opening up new variables, such as the date of TCM3, or by adding additional TCMs. Furthermore, the spacecraft's dry mass may be increased by launching into a parking orbit with a different inclination, depending on the performance of the launch vehicle.

DISCUSSION

The techniques studied in this paper may be used to construct a transfer from a particular state at the Earth to a particular low-energy lunar transfer. The results of this study are useful to help identify the costs associated with selecting a low-energy lunar transfer for a mission.

Studies such as those given in References 3–5 may be used to identify families of low-energy lunar transfers. Among those families there may be a few transfers that have desirable features, such as access to a region of the Moon or access to a particular area in the lunar vicinity. This paper provides information about the deterministic costs associated with connecting the low-energy lunar

transfer with a realistic trans-lunar injection. This information may be used to help identify which lunar transfers are more likely to work in a practical mission design before the mission designer spends much time studying the problem.

The surveys conducted to study Problem 2 have shown that it costs on the order of 1 m/s of additional ΔV per degree of inclination change between the LEO parking orbit and the geometry of the lunar transfer's natural Earth departure. Thus, if a mission will be launched from Cape Canaveral into a parking orbit that has an inclination of 28.5°, one can estimate the fuel cost of transferring from that orbit onto any given low-energy lunar transfer. The ΔV costs rise if the lunar transfer's departure geometry is close to equatorial. Additional surveys must be completed in order to characterize the statistical relevance of these findings. It is possible that the ΔV cost associated with changing a trajectory's inclination is dependent on the duration of the transfer or the number of phasing orbits and/or flybys the trajectory contains.

The results of analyses of Problem 2 have also shown that it requires on the order of 5 – 6 m/s more ΔV during the transfer per day of difference between the Earth departure date and the time that the low-energy lunar transfer naturally departs the Earth. This assumes that the transfer is constructed with one or two TCMs. By adding a third maneuver, it has been shown that this ΔV cost may be reduced. The two-burn and three-burn techniques have both been applied to the task of constructing a 21-day launch period for the reference mission. The two-burn technique requires approximately 73.6 m/s of ΔV; the three-burn technique requires only 56.0 m/s: a savings of approximately 17.6 m/s. The least expensive transfer for the reference mission requires approximately 14 m/s of ΔV in both launch periods; therefore, one can conclude that the reference mission's ΔV budget requires an allocation of approximately 59.6 m/s for the two-burn technique or 42.0 m/s for the three-burn technique. This study provides one data point for a mission designer; it must be repeated for many more low-energy transfers in order to establish an expected ΔV requirement for a launch period. It may be the case that certain types of low-energy transfers require more ΔV than others when the injection date is varied.

These results help provide guidance to mission designers attempting to understand how much deterministic ΔV will be included in a realistic low-energy lunar transfer.

CONCLUSIONS

The algorithms described in this paper generate low-cost transfers from specific low-Earth parking orbits to desirable low-energy lunar transfers. The technique involves separating the transfer problem into three trajectory segments and linking them with trajectory correction maneuvers. SNOPT has been found to be very useful at optimizing the systems studied in this paper, assuming that the optimizer is initialized with a good guess. Procedures are developed in this paper that have a high probability of generating an initial guess in the basin of attraction of the global best transfer.

A practical low-energy lunar transfer departs the Earth from a practical parking orbit, such as a 185-km circular orbit at an inclination of 28.5°. A desirable low-energy lunar transfer may naturally depart the Earth from some other inclination at a different time. This paper provides methods to estimate the deterministic ΔV cost of transferring from the practical LEO parking orbit onto the desirable low-energy lunar transfer. It has been found that a 21-day launch period requires on the order of 50 m/s of ΔV, depending on the trajectories. Furthermore, low-energy transfers that naturally depart the Earth at declinations far from the desired value, e.g., far from 28.5°, require approximately 1 m/s of additional ΔV per degree of difference. These costs are small compared to

the benefits that missions may receive by implementing a low-energy transfer to the Moon.

ACKNOWLEDGEMENTS

The research presented in this paper has been carried out at the Jet Propulsion Laboratory, California Institute of Technology, under a contract with the National Aeronautics and Space Administration.

REFERENCES

[1] S. B. Broschart, M. J. Chung, S. J. Hatch, J. H. Ma, T. H. Sweetser, S. S. Weinstein-Weiss, and V. Angelopoulos, "Preliminary Trajectory Design for the Artemis Lunar Mission," *AAS/AIAA Astrodynamics Specialist Conference*, No. AAS 09-382, Pittsburgh, Pennsylvania, AAS/AIAA, August 9–13, 2009.

[2] P. Xaypraseuth, "Gravity Recovery and Interior Laboratory (GRAIL) Project: Mission Plan," Tech. Rep. JPL D-38928, JPL, California Institute of Technology, 4800 Oak Grove Dr., Pasadena, CA 91109, November 2008.

[3] J. S. Parker, *Low-Energy Ballistic Lunar Transfers*. PhD thesis, University of Colorado, Boulder, Colorado, 2007.

[4] J. S. Parker and G. H. Born, "Modeling a Low-Energy Ballistic Lunar Transfer Using Dynamical Systems Theory," *Journal of Spacecraft and Rockets*, Vol. 45, No. 6, 2008, pp. 1269–1281.

[5] J. S. Parker, "Low-Energy Ballistic Transfers to Lunar Halo Orbits," *AAS/AIAA Astrodynamics Specialist Conference*, No. AAS 09-443, Pittsburgh, Pennsylvania, AAS/AIAA, August 9–13, 2009.

[6] W. S. Koon, M. W. Lo, J. E. Marsden, and S. D. Ross, "Shoot the Moon," *AAS/AIAA Spaceflight Mechanics 2000*, Vol. 105, part 2, AAS/AIAA, 2000, pp. 1017–1030.

[7] E. A. Belbruno and J. Miller, "A Ballistic Lunar Capture Trajectory for the Japanese Spacecraft Hiten," Tech. Rep. IOM 312/90.4-1731-EAB, JPL, California Institute of Technology, 1990.

[8] E. A. Belbruno, "Lunar Capture Orbits, a Method of Constructing Earth Moon Trajectories and the Lunar Gas Mission," *The 19th AIAA/DGLR/JSASS International Electric Propulsion Conference*, No. AIAA 87-1054, Colorado Springs, Colorado, May 1987.

[9] E. A. Belbruno, *Capture Dynamics and Chaotic Motions in Celestial Mechanics*. Princeton University Press, Princeton, NJ, 2004.

[10] V. V. Ivashkin, "On Trajectories of the Earth-Moon Flight of a Particle with its Temporary Capture by the Moon," *Doklady Physics, Mechanics*, Vol. 47, No. 11, 2002, pp. 825–827.

[11] V. V. Ivashkin, "On the Earth-to-Moon Trajectories with Temporary Capture of a Particle by the Moon," *54th International Astronautical Congress*, No. Paper IAC-03-A.P.01, Bremen, Germany, Sept. 29–Oct. 3, 2003, pp. 1–9.

[12] V. V. Ivashkin, "On Particle's Trajectories of Moon-to-Earth Space Flights with the Gravitational Escape from the Lunar Attraction," *Doklady Physics, Mechanics*, Vol. 49, No. 9, 2004, pp. 539–542.

[13] V. Szebehely, *Theory of Orbits: The Restricted Problem of Three Bodies*. New York: Academic Press, 1967.

[14] J. S. Parker and M. W. Lo, "Shoot the Moon 3D," *AAS/AIAA Astrodynamics Specialist Conference*, No. AAS 05-383, Lake Tahoe, CA, AAS/AIAA, August 7–11, 2005.

[15] R. Wilson, "Derivation of Differential Correctors Used in GENESIS Mission Design," Tech. Rep. JPL IOM 312.I-03-002, Jet Propulsion Laboratory, California Institute of Technology, 2003.

[16] K. C. Howell and H. J. Pernicka, "Numerical Determination of Lissajous Trajectories in the Restricted Three-Body Problem," *Celes. Mech.*, Vol. 41, 1988, pp. 107–124.

[17] K. C. Howell, "Three-Dimensional, Periodic, 'Halo' Orbits," *Celes. Mech.*, Vol. 32, No. 1, 1984, pp. 53–71.

[18] P. E. Gill, W. Murray, and M. A. Saunders, "User's Guide for SNOPT 7.1: A Fortran Package for Large-Scale Nonlinear Programming," Tech. Rep. Numerical Analysis Report NA 04-1, Department of Mathematics, University of California, San Diego, La Jolla, CA, 2004.

[19] P. E. Gill, W. Murray, and M. A. Saunders, "SNOPT: An SQP Algorithm for Large-Scale Constrained Optimization," *SIAM Review*, Vol. 47, No. 1, 2005, pp. 99–131.

APPENDIX A: AVOIDING RIDGES IN THE STATE SPACE

The purpose of this section is to show why a perturbed state improves SNOPT's ability to find an improved solution in the parameter space that corresponds with Problems 2 and 3 described in this paper.

The first three steps of the four-step process that is used to construct good initial guesses to Problem 2 often yield a solution where Segment 1 intersects Segment 3 in position space within some small tolerance level. It has been observed that SNOPT often has difficulty moving away from that state even when there is a much deeper minimum in the same basin of attraction. The hypothesis is that the objective function space is very flat in the vicinity of one of these solutions.

Although the SNOPT algorithm computes the Jacobian matrix of system, one can visualize the surface of the local state space by estimating the values of the partial derivatives $\partial \Delta \mathrm{V} / \partial p$, where p is one of the parameters of interest, namely, $p \in \{ \Omega_L, \nu_L, \Delta \mathrm{V}_L, \Delta t_1, \Delta t_2 \}$. In this discussion these partial derivatives are computed numerically. They are only accurate within a small vicinity around a solution.

Table 4 displays the values of the components of $\mathbf{X_2}$ as it is constructed through the four-step process. If the process is terminated after three steps, then $\mathbf{X_2}$ contains the following parameters:

$$\begin{aligned} \mathbf{X_2} &= \{ \Omega_L, \nu_L, \Delta \mathrm{V}_L, \Delta t_1, \Delta t_2 \} \\ &= \{ 119.64^\circ, 36.71^\circ, 3212.52 \text{ m/s}, 20 \text{ days}, 20 \text{ days} \} \end{aligned}$$

The resulting Segment 1 intersects Segment 3 in position space within approximately 4 cm at the time of TCM1. The total transfer ΔV for that parameter set is equal to approximately 28.39 m/s and TCM1 performs almost all of the work.

If the initial guess algorithm completes the fourth step, then one obtains the perturbed parameter set $\hat{\mathbf{X}}_\mathbf{2}$:

$$\begin{aligned} \hat{\mathbf{X}}_\mathbf{2} &= \{ \Omega_L, \nu_L, \Delta \mathrm{V}_L, \Delta t_1, \Delta t_2 \} \\ &= \{ 119.64^\circ, 36.71^\circ, 3212.52 \text{ m/s}, 21 \text{ days}, 21 \text{ days} \} \end{aligned}$$

The partial derivatives may be numerically computed by perturbing each parameter and observing the resulting change in the transfer's ΔV. Table 11 captures the numerical partials using both parameter sets $\mathbf{X_2}$ and $\hat{\mathbf{X}}_\mathbf{2}$. Most of the partials of $\mathbf{X_2}$ are nearly zero; furthermore, the nearby slopes are convex: the only way the optimizer can improve the system is by moving in the direction of Ω_L. Whereas each and every partial near $\hat{\mathbf{X}}_\mathbf{2}$ is nonzero, indicating that the optimizer can easily move toward an improved minimum in the state space. It's certainly possible that the optimizer will encounter the flat area around $\mathbf{X_2}$, but the perturbation grants the optimizer more mobility. All empirical evidence indicates that this mobility helps the optimization process.

Table 11. The numerical partials for the parameter sets $\mathbf{X_2}$ and $\hat{\mathbf{X}}_\mathbf{2}$.

Parameter	$\mathbf{X_2}$	$\hat{\mathbf{X}}_\mathbf{2}$
$\partial\Delta\mathrm{V}/\partial\Omega_L$	$\sim$0.26 m/s/deg	$\sim$23.5 m/s/deg
$\partial\Delta\mathrm{V}/\partial\nu_L$	$\sim$0.0 m/s/deg	$\sim$11.2 m/s/deg
$\partial\Delta\mathrm{V}/\partial\Delta\mathrm{V}_L$	$\sim$0.0	$\sim$-1.36
$\partial\Delta\mathrm{V}/\partial\Delta t_1$	$\sim$0.0 m/s/day	$\sim$2.63 m/s/day
$\partial\Delta\mathrm{V}/\partial\Delta t_2$	$\sim$0.0 m/s/day	$\sim$-0.13 m/s/day